N. Mehendale et al., International Journal of Advanced Research in Computer Science and Software Engineering 3(10), October - 2013, pp. 1-8

Cell path tracking in microfluidic cell sorting chip using image processing

Ninad D. Mehendale*
Department of Biosciences & Bioengineering,
Indian Institute of Technology Bombay
ninad.mehendale@gmail.com

Khushal Kharade*
Department of Electrical Engineering,
Indian Institute of Technology Bombay
allkhush92@gmail.com

Kaustubh Chhabilwad*
Department of Electrical Engineering,
Indian Institute of Technology Bombay
chhabilwadkaustubh@gmail.com

Dr. Debjani Paul
Department of Biosciences & Bioengineering, Indian Institute of Technology Bombay
debjani.paul@iitb.ac.in

Dr. Shabbir N. Merchant
Department of Electrical Engineering,
Indian Institute of Technology Bombay
merchant@ee.iitb.ac.in

Abstract— This paper shows implementation of image processing algorithm used for automated cell path tracking in a microfluidic cell sorting device. Nowadays point of care diagnostics is becoming popular, there exist a need for microfluidic lab on a chip device which is portable and should be able to perform all the functions of a pathology lab. One of the applications of pathology lab is "cell path tracking", which we demonstrate in this work. Cell path tracking allows user to get accurate counts of sorted cells, to separate live and dead cells, to predict next location of the cell, so that proper drug delivery can be done. This image processing is done on bright field images obtained from frames of videos and do not require any external tagging. This algorithm is video frame rate independent. The cell path is tracked by simple morphological operations and some spatial domain operations such as image subtractions.

Keywords— Microfluidics, Cell sorting, Path tracking, Image processing, Automatic path predictions

I. INTRODUCTION

This paper aims at tracking the cell path in a video obtained by microscope. Microfluidics is study of fluid flow of order of few Nano litre – Pico litre through structures of order of few orders of micrometres. Cell sorting microfluidic device is made up of pillar rows with gap size reducing in five successive stages. Fluorescent labelling and confocal microscopes [1] are generally used to detect the cells with ease. But fluorescent labelling cells may affect cell behaviour. In the present work we do not label cells via any fluorescent label such as fluorophore. Although 3D path tracking of motile bacteria using tracking microscope [2] was shown in 1995 by Frymier and his group but equation of tracked bacteria was evaluated. In our work after tracking the path of cell we evaluate equation by n^{th} order curve fitting where 'n' is number of frames extracted. Feature point tracking[3] for cells using computational methods were demonstrated by Sbalzarini and his group but in our approach we select flowing cells due to syringe pressure applied at the input unlike freely suspended cells. Debeir and group established migrating cell trajectories in phase contrast microscopy[4]. In our work we have used bright field images to establish path of cells. Path tracking is useful in quantitative analysis of chemotaxis[5]. Although two photon microscope [6] proved very useful in background removal, we use image subtraction and then thresholding which provides fair amount of background removal.

Cell path tracking is useful in stem cell therapies [7]. Recently Cell path tracking algorithm needs to be developed for Android / iPhone for point of care devices using microfluidics. Cell path tracking allows user to get exact count of cells avoiding multiple count for same cell. Speed of cell and capacity of cell to swim against flow is direct indicator of cell's health and growth cycle. Even live and dead cells could be determined by cell path tracking, as the dead cells tend to flow along the laminar flow of channel; but live cells will have some variation. The algorithm developed is independent of frames per second.

II. METHODS

Device is designed with five pillar rows. In each corresponding row pillar spacing goes on reducing. Each pillar is of size 200*200 µm. Spacing for five pillar rows are 100, 50, 20, 10, 5µm respectively from left to right. Steps followed to fabricate microfluidic device used in our experiment are described below:

A. Mask Preparation

Microfluidic cell sorting device was designed using AutoCAD 2012 student version as shown in Fig. 1. The Fig. 1 shows outer circular boundary of 2 inch Silicon wafer. There are total 3 inputs on the left. Centre input is sample input from which mixed population of cells are passed and other two inputs are for buffer solution. There are 6 outlets for each kind of cells. Cells of small size can go through all pillar stages; but the bigger cells will be blocked and they will come out via outlet just before the pillar row that particular cell could not pass through. The device was simulated in COMSOL version 4.3b. After testing device layout was converted as mask by printing it onto a transparent film.

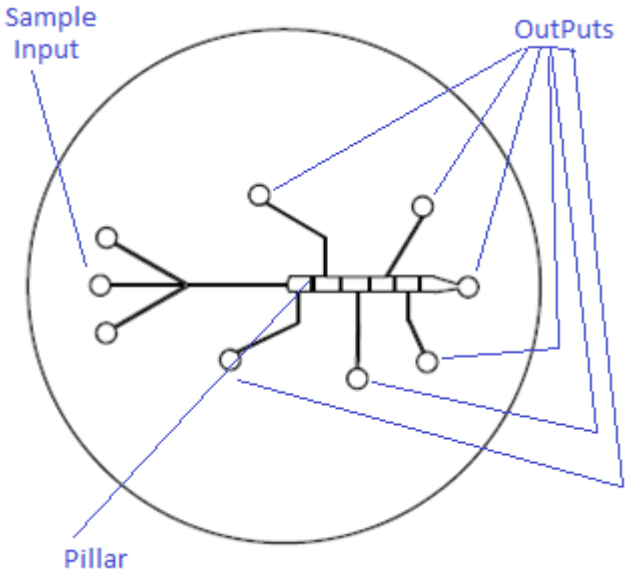

Fig. 1 AutoCAD mask having one sample input in the centre and two buffer input from sides.
Six outputs to collect sorted cells before and after each pillar row.

The printed transparency is then attached with 3*3 inch optically polished glass slide as shown in Fig.2. Actual mask prepared was measured with Olympus microscope with 10X objective. It is observed that up to 25µm variation exist in mask and prepared AutoCAD dimensions. Fig.2 shows part of the mask, where only three pillar rows out of five and three outlets are visible. Leftmost pillar row has spacing of 20µm. Middle row has spacing of 10µm and rightmost has pillar spacing of 5µm.

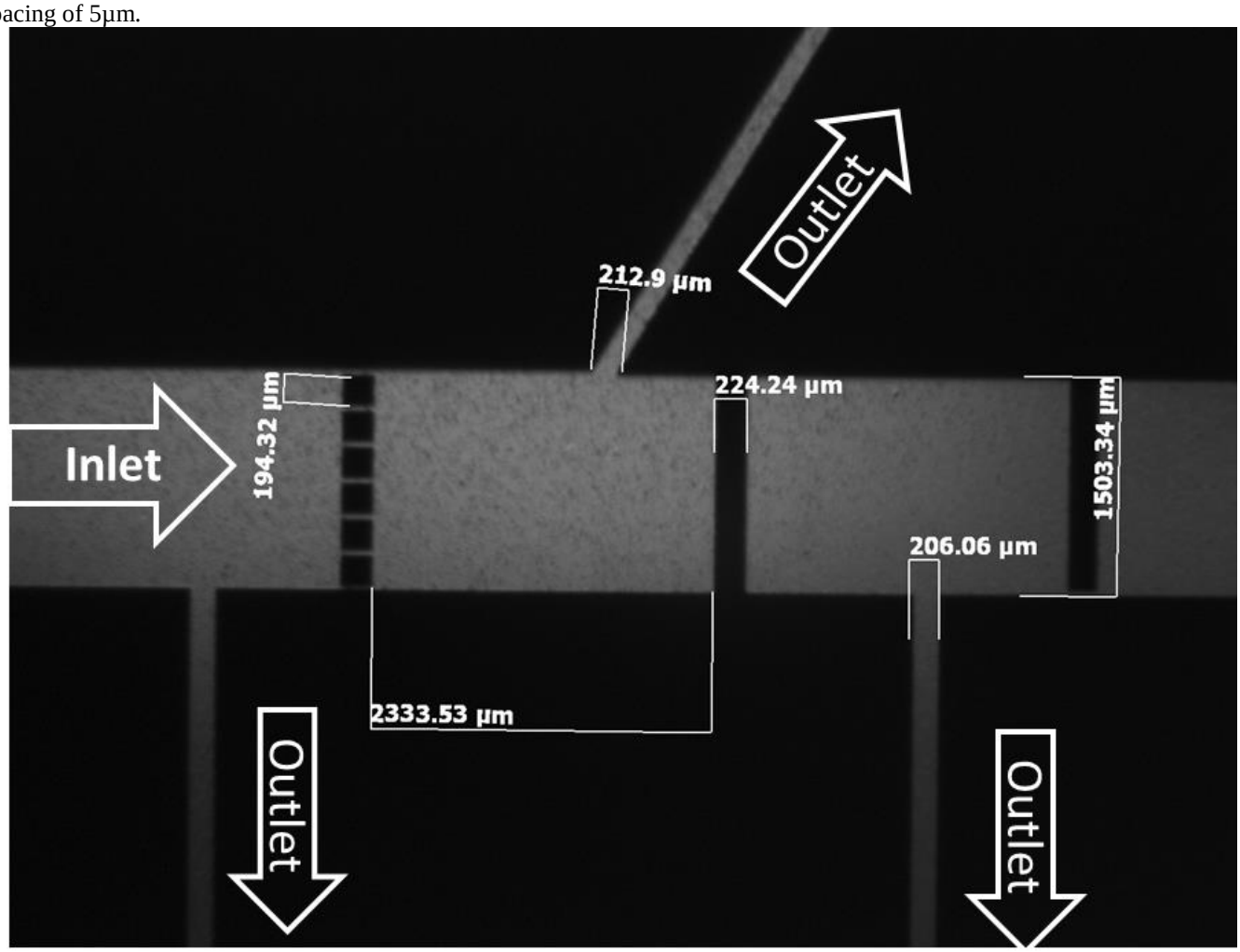

Fig. 2 Actual mask prepared having different dimensions and showing inlet and outlet has variances of 25µm

B. Master Preparation

Master is prepared on 2 inch Silicon wafer which is RCA cleaned. RCA cleaning is done by dipping single sided polished Silicon wafer into NH_4O_4 (Ammonium hydroxide) + H_2O_2 (Hydrogen peroxide) + H_2O (Water) in the ratio 1:1:5. Step 2 of RCA called 'HF dip', where Silicon wafer is kept in HF+H_2O in ratio 1:50 for 3 min. In the 3rd and final step HCL+ H_2O_2 (Hydrogen peroxide) + H_2O (Water) in 1:1:6 ratio to remove any metallic contaminant.

RCA clean wafer is coated with SU8 2025 which is negative photoresist. 2025 specifies at 25 micron height when spin-coated at 3000rpm for 45 sec with 15 sec pre-acceleration at 500 rpm. This RCA cleaned wafer is prebaked at 65 degrees for 3 min and then exposed to UV light in Karl-Suss mask aligner MJB-3 for 45 sec. RCA wafer is post baked at 95 degrees for 1 min and dipped in SU-8 developer for 5 min. Fig. 3 shows picture of master.

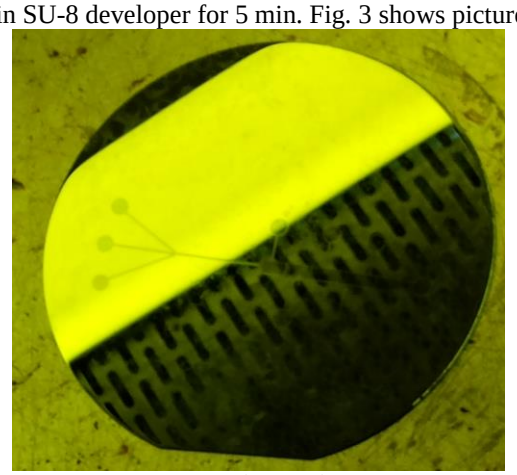

Fig. 3 Master prepared using SU8 after transferring the pattern on mask

C. Device Making

Once the master is prepared it acts like a negative of required pattern and multiple devices can be peeled off from the master. Actual device is made up of PDMS (polydimethylsiloxane) mixed as 10:1 ratio base to curing agent. After degassing using desiccator PDMS is poured onto the master kept in glass Borosil petri dish. Petri dish is then kept in oven at 65 degrees for 45 minutes. Once cures PDMS is peeled off and cut by sharp knife. Holes of 1.5mm for inlet are drilled with biopsy punch. Glass cover slip of 24*60mm is used as the base of the device. Glass cover slip is preferred over glass slide since glass cover slip is better for imaging especially when oil immersed imaging is done at 100X. Piranha cleaning glass cover slip is done with mixture of sulphuric acid (H_2SO_4) and hydrogen peroxide (H_2O_2) at 3:1 ratio. PDMS device after cleaning with scotch tape and piranha cleaned glass cover slip both are kept inside plasma cleaner. We have used Harrick plasma cleaner with O_2. Plasma is created for 90 seconds which converts hydrophobic region of PDMS to hydrophilic allowing creating irreversible bonding between glass and PDMS. Fig. 4 shows final device prepared having six outlets and three inlets.

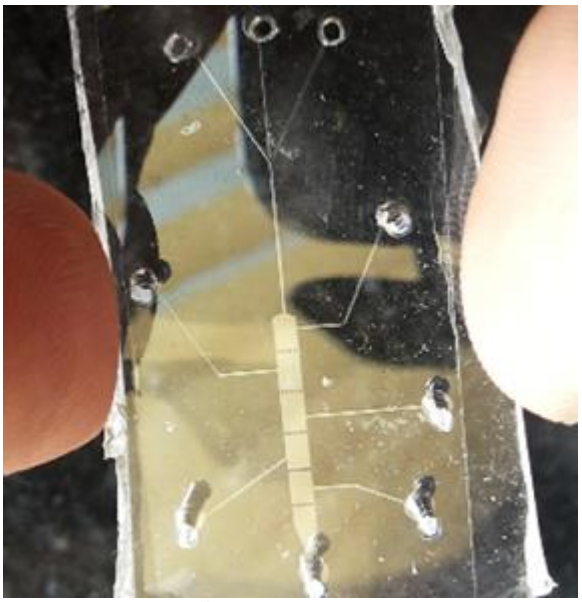

Fig. 4 Final microfluidic cell sorting device prepared

The device is then connected with microfluidic connectors and syringe of 5ml to syringe pump. Flow rate is set to 10 µl/min.

III. IMAGE PROCESSING ALGORITHM

A. Resizing the image

The entire image obtained is resized to 25% in order to improve speed of execution. This is done by removing every alternate pixel from rows and then from column. This operation also referred as image scaling. There is a trade-off between speed of execution and few image details such as smoothness, sharpness etc. in image resizing.

B. Image subtraction

Image subtraction in spatial domain is process of subtracting pixel of previous image from pixel of current image. This process will remove any stationary background and only keep the moving objects in the image. Robust image subtraction algorithm is achieved by subtracting unsigned values and taking modules of the answer.

$$D(x,y,t) = |V(x,y,t) - V(x,y,t-1)| \quad (1)$$

Equation (1) shows generalized image subtraction that is implemented in our algorithm where D(x,y,t) is the difference image, V(x,y,t) is the current image and V(x,y,t-1) is previous image. V stands for frame in video and D stands for difference.

C. Histogram calculation

Histogram of any image is plot of all grey levels verses the number of times that particular grey level appears in the picture frame. Generally images are stored in 8 bits per pixel hence x-axis of histogram is from 0 to 255 (2^8-1).

$$P(r_k) = n_k / n \quad (2)$$

Equation (2) shows probability or normalized histogram where n is total number of pixels n_k is number of times level r_k occurs and r_k is the k^{th} level in between 0 to 255. Sum of all the components in normalized histogram is always one. It gives global information about the picture but cannot give exact position of the pixel in picture. It also gives information about distinct regions in image which will help in thresholding. Each region is called 'mode'. Histogram of two images can be exactly same hence histogram is not unique for each image.

D. Histogram stretching

Histogram stretching is also referred as contrast stretching, where dynamic range of grey level intensities is stretched from 0 to 255. Equation (3) shows histogram stretching of an image having dynamic range in between c and d to a and b; Where c is original image`s lowest grey level value, d is original image`s highest grey level value, b is desired higher level i.e.255 in this case and a is desired low level i.e. 0 in this case. We assume that a < c and b>d. P_{in} is current pixel value and P_{out} is new value.

$$P_{out} = (P_{in} - c) * (b - a / d - c) + a \quad (3)$$

E. Morphological image processing

Morphology is branch of biology that deals with the form and structure of plants and animals. In image processing 'mathematical morphology' is used as tool for extracting image components that are useful in the representation and description of regions and shapes of an image. Mathematical morphology may be explained using set theory. Sets in mathematical morphology represent objects in an image. In binary images, the sets are members of the 2-D integer space Z^2, where each element of a set is tuple (2-D vector) whose co-ordinates are the (x, y) co-ordinates of black pixel in an image. Grey scale images can be represented as sets whose components are in Z^3.

Image opening is dilation followed by erosion of image A by structuring element B. In simple words, morphological opening will open the small gaps in to wide gaps. Image opening 'o' is represented as,
$A \circ B = (A \ominus B) \oplus B$, Where $\ominus$ indicates erosion and $\oplus$ indicates dilation.

Image closing is operation of erosion followed by dilation of image A by structuring element B, Image closing allows to close small gaps to enclosed structures e.g. C shape will become O shape. Image closing '$\bullet$' is given by,
$A \bullet B = (A \oplus B) \ominus B$, Where $\ominus$ indicates erosion and $\oplus$ indicates dilation.

Dilation operation basically expands the shape of the existing object by structuring element used. It is somewhat similar to drawing outer boundary across all edges.

F. Connectivity of two pixels

If two pixels are said to be connected, they must be neighbours and their grey levels should satisfy a specified criterion of similarity. For example, in a binary image with values 0 and 1, two pixels may be neighbours, but they are said to be connected only if they have same value. e.g. 00 and 11 are connected but 01 and 10 are not connected but they are neighbours. In short all the connected pixels are neighbouring pixels but not all neighbouring pixels are connected.

G. Algorithm

Different steps in image processing include:

- Image resizing for all n images.
- Subtraction of two images i.e. current image – previous image.
- Averaging of all subtracted (n-1) images.
- Histogram calculation.
- Histogram stretching.
- Image thresholding.
- Image morphological closing.
- Image morphological opening.
- Image dilation.
- Image morphological closing.
- Image morphological opening.
- 4 connected neighbouring pixels.
- Minimum Euclidean distance between the pixels.
- Area verification by 8 connected pixels.
- Polynomial fitting of nth order.

IV. RESULTS AND DISCUSSIONS

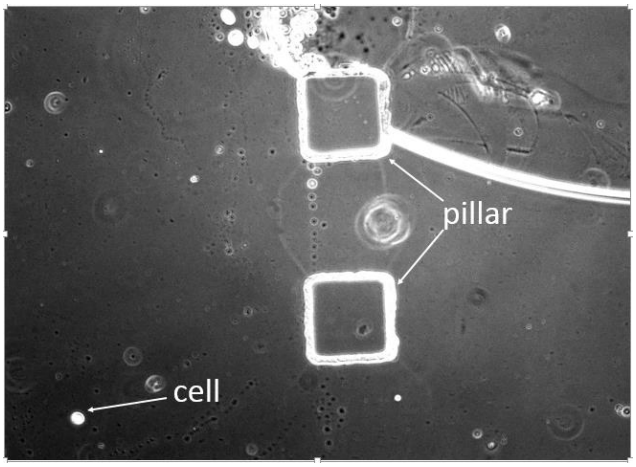

Fig. 5(a) Input image

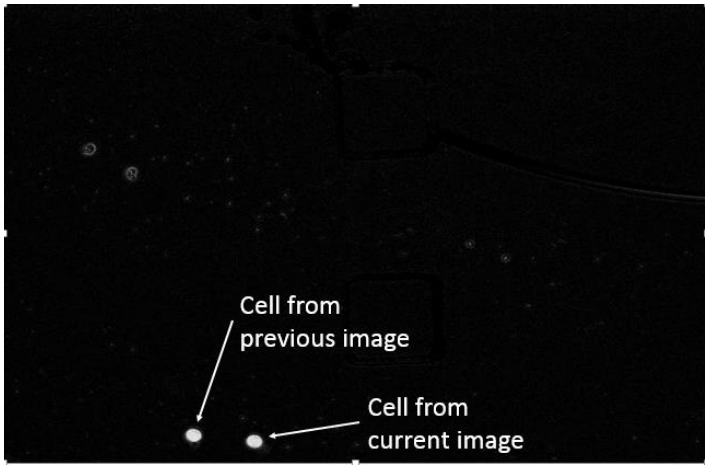

Fig. 5(b) Image after subtraction

Fig. 5(a) shows original input frame consisting of a cell and two pillars at 10X zoom and flow of the liquid is from left to right. Fig. 5(b) shows result after image subtraction. As the background is same for current and previous image only the difference is enhanced that is the moving objects.

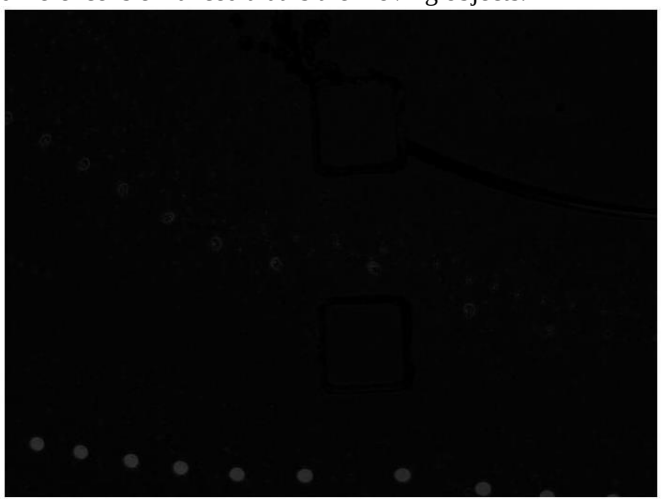

Fig. 6(a) Image after averaging all difference images

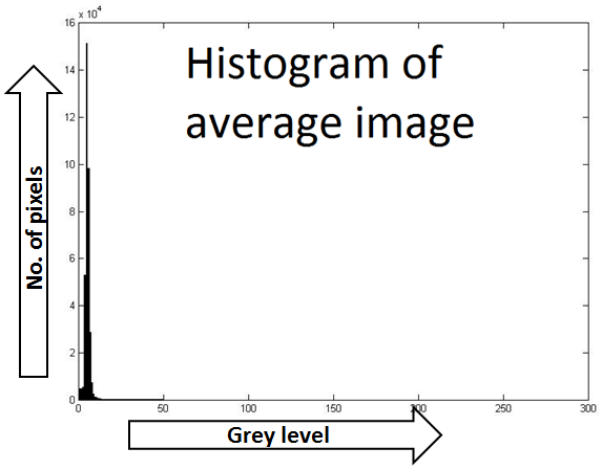

Fig. 6(b) Histogram of average image

Fig. 6(a) shows the average output of all the background subtracted images. Fig. 6(b) shows histogram of averaged image. The output is very low contrast image as most of the levels are towards zero and dynamic range is also very low.

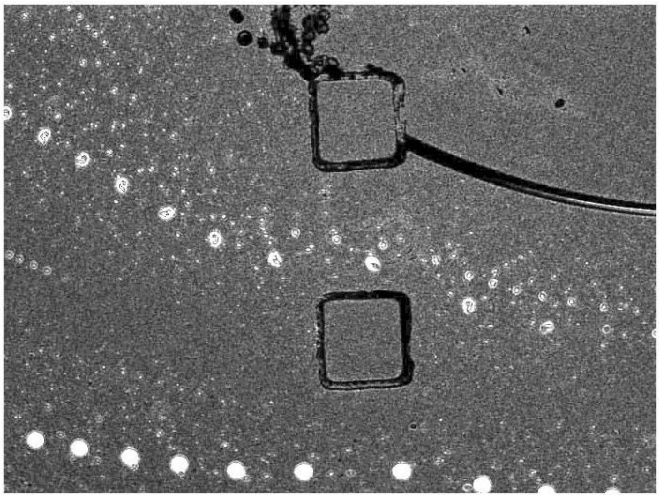

Fig. 7(a) Histogram stretched image

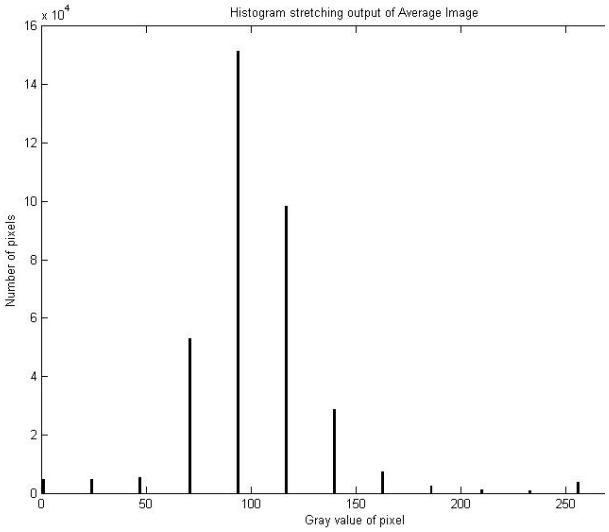

Fig. 7(b) Histogram after stretching

Fig.7(b) shows contrast stretched histogram and its corresponding improved image is shown in fig. 7(a).

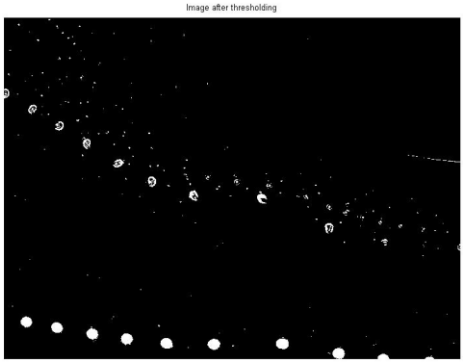

Fig. 8(a) Image after thresholding

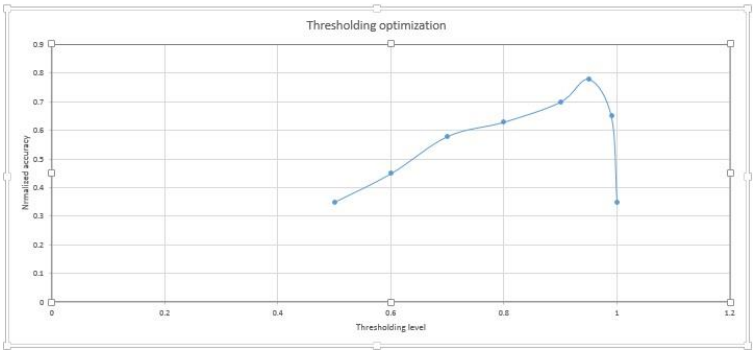

Fig. 8(b) Optimization of thresholding value.

Fig. 8(a) shows result of image thresholding when the value is 95% of maximum. Fig. 8(b) shows graph of optimization of threshold value varying from 0.5 to 1. It is found that peak occurs at 0.95.

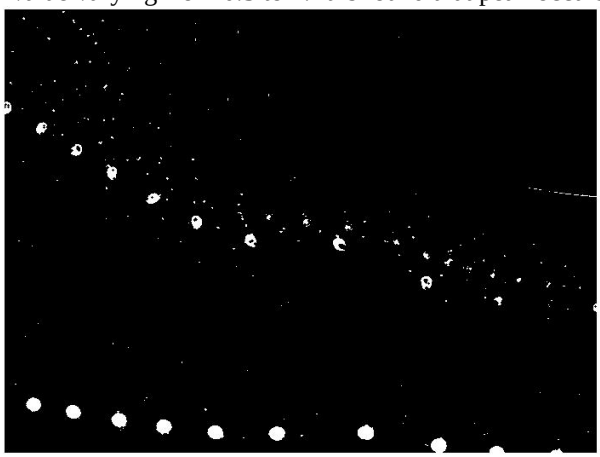

Fig. 9(a) Image after first morphological closing after thresholding

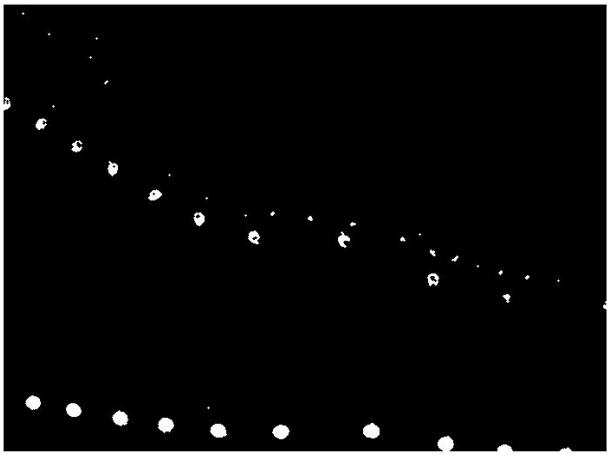

Fig. 9(b) Image after morphological opening

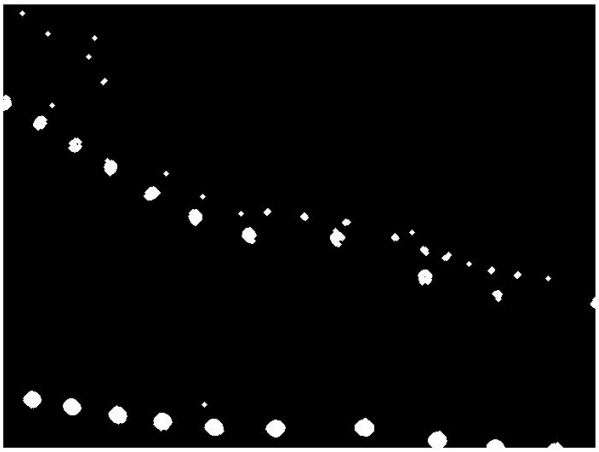

Fig. 9(c) Image after dilation

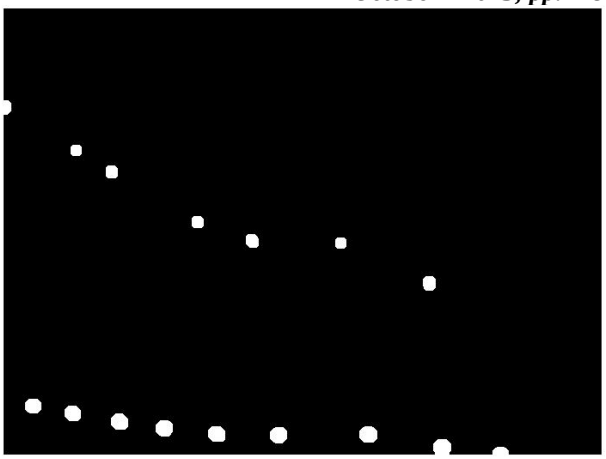

Fig. 9(d) Image after second morphological closing

Fig. 9(a) shows output of morphological closing after thresholding. Empty pixels in encloses environment is filled with white pixels. Fig. 9(b) shows result after morphological opening where small noisy pixels are eliminated. Fig. 9(c) shows result after dilation where image is smoothened out and successive closing is shown in Fig.9(d) for any unwanted noise to reduce. Lastly image opening is performed, which results only in existence of desired cells and all other noise are being successfully removed. Fig. 10 shows the final tracked path fitting 3rd order polynomial equation. The equation is given by Y = (0.0228936858845234)X2 –(17.6890904545680)X + (3342.89135524076)

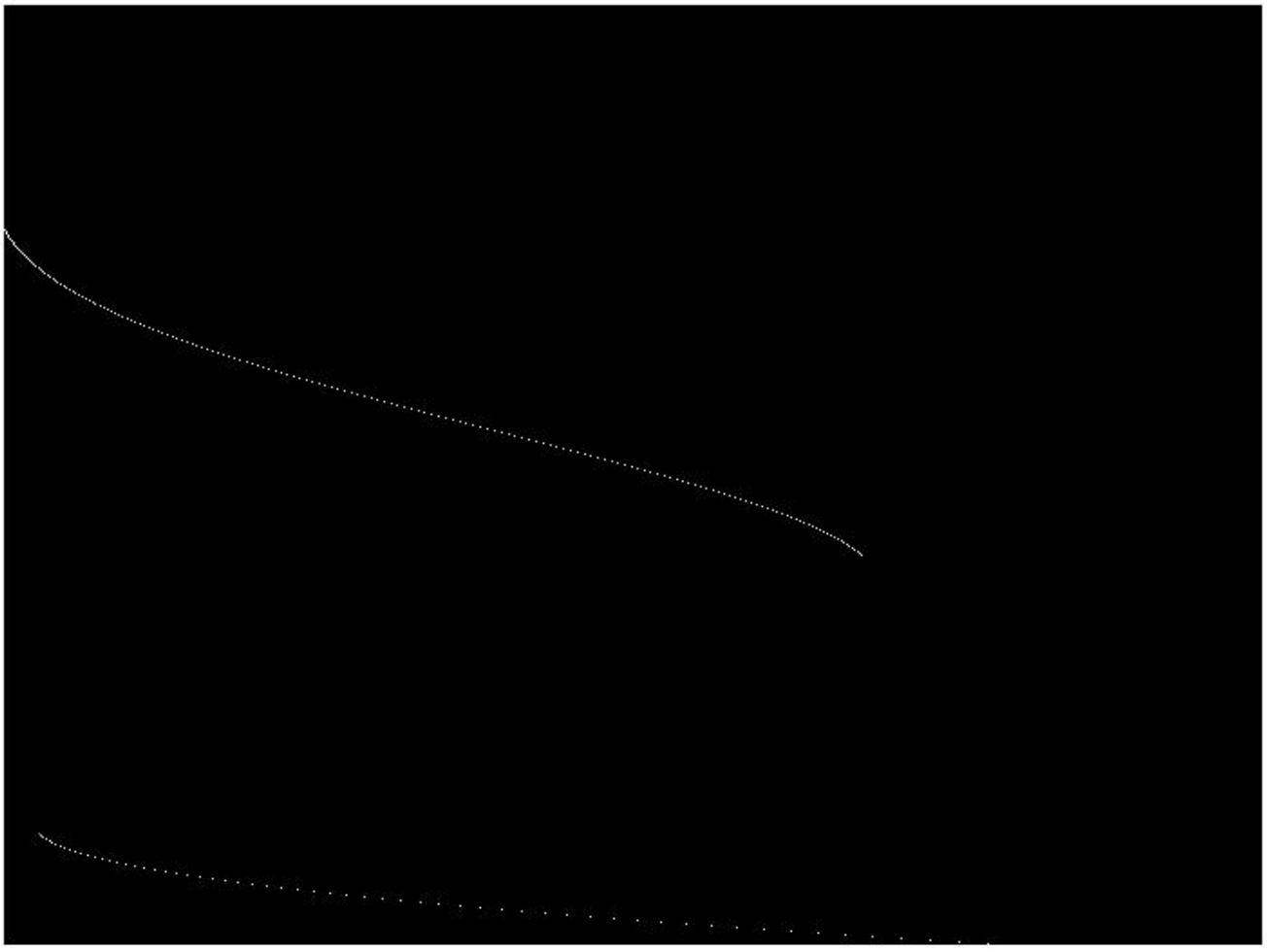

Fig. 10 Final output with cell tracked path

TABLE I

	Cell Path tracking algorithm results			
	Number of Frames	**Time (seconds)**	**Accuracy**	**Average and Standard deviation**
Video 1	11	132	1	88.4% ± 8.08%
Video 2	25	210	0.97	
Video 3	37	307	0.85	
Video 4	44	351	0.86	
Video 5	57	409	0.74	

Table 1 shows that as number of frames increases the average accuracy of this path tracking algorithm reduces. The average accuracy of this algorithm without modification to any parameters is around 88.4% with standard deviation of 8.08%. Table also shows average time is about 8.77±1.29 seconds/ frame. Generally number of frames required for one cell to pass through the field of view of microscope is about 12 frames at 10µliter/min with 500µm channel width and hence within 2 minutes the result will be calculated.

$$Y = (7.32219441107338e\text{-}25)X^{11} + (-1.48181383471587e\text{-}21)X^{10} + (1.13434018815318e\text{-}18)X^{9} + (-3.88067627822058e\text{-}16)X^{8} + (4.99396418834267e\text{-}14)X^{7} \quad (4)$$

Equation (4) shows 11^{th} order curve fitting for video 1 with 11 frames. It is observed from above equation only five coefficients of higher order elements exist and rest all coefficients are zero. Using this equation user can easily find x, y coordinates of the cell in an image.

V. CONCLUSIONS AND FUTURE SCOPE

The algorithm fits the curve and detects the path of the cell. It also predicts what could be the future locations of cell. Algorithm gives robust results with very high accuracy without modifying parameters selected. The further improvement in accuracy can be achieved by varying parameters of algorithm as per the video parameters. The algorithm is also useful in predicting the path of the particle by adjusting thresholds.

ACKNOWLEDGMENT

We would like to thank Indian Institute of Technology Bombay for the infrastructure and facilities provided for the experiment. We would like to express our sincere gratitude to our HOD Dr. Rohit.Manchanda(BSBE department) and Dr. Abhay karandikar (EE department) and our lab mates Ammar, Tanvir, Prasad, Siddartha and Sampath. The authors would like to thank all our colleagues at IITB. We want to thank Dr. Shamik sen and Alkesh for all the microscope images. We thank Prof. Rajdip from chemical engineering department of IITB for the kind support he provided.

REFERENCES

[1] Godbey W. T., Kenneth K. Wu, and Antonios G. Mikos, "Tracking the intracellular path of poly (ethylenimine)/DNA complexes for gene delivery." Proceedings of the National Academy of Sciences 96.9 (1999): 5177-5181.

[2] Frymier, Paul D., et al. "Three-dimensional tracking of motile bacteria near a solid planar surface." Proceedings of the National Academy of Sciences 92.13 (1995): 6195-6199.

[3] Sbalzarini, Ivo F., and Petros Koumoutsakos. "Feature point tracking and trajectory analysis for video imaging in cell biology." Journal of structural biology 151.2 (2005): 182-195.

[4] Debeir, Olivier, et al. "Tracking of migrating cells under phase-contrast video microscopy with combined mean-shift processes." Medical Imaging, IEEE Transactions on 24.6 (2005): 697-711.

[5] Fisher, P. R., Rainer Merkl, and G. Gerisch. "Quantitative analysis of cell motility and chemotaxis in Dictyostelium discoideum by using an image processing system and a novel chemotaxis chamber providing stationary chemical gradients." The Journal of cell biology 108.3 (1989): 973-984.

[6] Levi, Valeria, QiaoQiao Ruan, and Enrico Gratton. "3-D particle tracking in a two-photon microscope: application to the study of molecular dynamics in cells." Biophysical journal 88.4 (2005): 2919-2928.

[7] Cyranoski, David. "Japan to offer fast-track approval path for stem cell therapies." Nature medicine 19.5 (2013): 510-510.

